

Influence of Platform Scattering on W-Band CubeSat Missions

Tonny Rubæk, Jakob Rosenkrantz de Lasson, Cecilia Cappellin, Oscar Borries
TICRA, Landemærket 29, DK-1119 Copenhagen K, Denmark, ticra@ticra.com

Abstract—A W-band reflector antenna mounted in a 6-unit CubeSat is analysed. The analyses show that the effects of the CubeSat structure on the performance of the antenna are significant, both on the peak gain and side-lobe levels while the impact on XPD performance is less significant.

I. Introduction

As the CubeSat platform [1] matures, the interest in flying more advanced payloads using increasingly high frequencies for the payload antennas is rising – both for data-download and for scientific missions [2]. As the frequency increases, the electrical sizes of both the antennas and the CubeSat platform increases while the beamwidth decreases. Whereas the commonly applied S- and L-band antennas have broad beams and only experience small impacts from the presence of the CubeSat platform, the effect on the antenna performance at higher frequencies can be significant and must be taken into account in details when designing the antennas.

In this work, we present an analysis of the scattering from a CubeSat platform for a reflector-antenna system in W band. We compare the pattern of the antenna on its own with that of the antenna mounted in a 6-unit (6U) CubeSat and illustrate the impact of the platform scattering for a realistic system configuration.

The RF analyses are carried out using the MoM/MLFMM solver in ESTEAM from TICRA Tools 19.0 [3]. This discretises the geometry using higher-order quadrilateral patches and surface currents using higher-order basis functions. This combination makes it particularly suited for electrically large structures, and its feasibility for conventional telecommunication satellites has already been demonstrated at lower frequencies [4].

II. Antenna configurations

We consider an offset reflector intended for CubeSat applications, inspired by [5], with projected aperture diameter of $D = 10$ cm, normalized focal length of $f/D = 0.25$ and no clearance (offset = $\frac{D}{2}$). The diameter of 10 cm and the relatively small focal length ensures that the antenna can fit inside the 6U CubeSat chassis as shown in Fig. 1. We consider a W-band frequency of 86 GHz, at which the CubeSat chassis has outer dimensions of $(29, 57, 86)\lambda$. We use a left-hand circularly (LHC) polarized tapered waveguide with aperture diameter of 3.2 mm as feed to achieve right-hand circular (RHC) polarization in the far-field of the reflector.

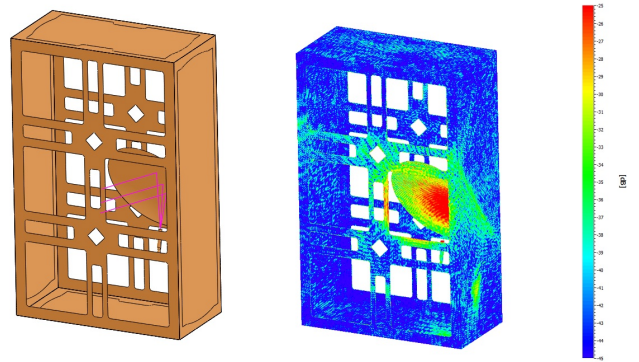


Fig. 1. Single-offset reflector antenna inside 6U CubeSat chassis (the front and back panels have been removed to give a better view of the antenna). Left: Reflector and open CubeSat chassis. Right: Simulated MoM currents on reflector and opened CubeSat chassis at 86 GHz.

Two antenna configurations are considered in this paper: To get a baseline performance for the antenna, we have first model the antenna on its own, i.e., with no CubeSat platform is present. This baseline performance is compared to the performance of the antenna when it is mounted in a closed CubeSat body. When mounted in the CubeSat, the antenna is oriented in such a way that the bore-sight direction of the antenna is perpendicular to the front surface of the antenna. All results are given in a coordinate system, which has its centre at the centre of the reflector and its z axis pointing in the direction of the bore sight. The x axis is pointing towards the feed.

The two configurations are showed in Fig. 2. In the configurations shown in this figure, the z axis of the coordinate system used for describing the results is oriented towards the reader while the x axis is oriented towards the bottom of the figure (along the long axis of the CubeSat platform).

The simulations of the two configurations require 1.2 gigabytes of memory for the antenna alone and 17 gigabytes for the antenna installed in the CubeSat platform.

III. Results

The influence of the platform scattering on a number of key parameters is now investigated. These parameters are: Peak directivity, side-lobe levels, and XPD. A comparison of the radiation patterns for the antenna alone and

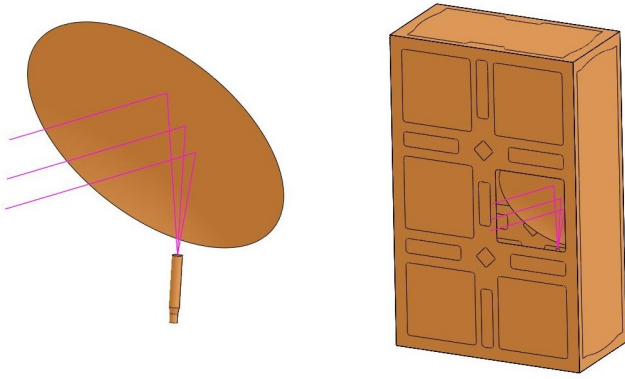


Fig. 2. Left: Reflector and tapered waveguide feed. Right: Antenna mounted inside closed CubeSat platform.

TABLE I

Peak directivity (in dBi) for antenna alone and antenna mounted in CubeSat platform.

	$\phi = 0^\circ$	$\phi = 45^\circ$	$\phi = 90^\circ$
Antenna	36.54	37.00	37.42
Antenna mounted in platform	35.01	35.33	35.69

mounted in the CubeSat platform are shown in Fig. 3. The cuts are shown for $\phi = 0^\circ$ (along the long axis of the platform), $\phi = 45^\circ$, and $\phi = 90^\circ$ (along the short axis of the platform).

A. Peak directivity

In Fig. 3 it is seen that mounting the platform in the CubeSat platform reduces the peak directivity significantly. For both configurations, the beam squint caused by using circular polarization is visible as a shift of the beam peak along the y axis of the system ($\phi = 90^\circ$ cut). The beam squint is the same with and without the platform present.

The peak directivity in the three cuts for the two different configurations are listed in Table I. The peak decreases from 37.42 dBi to 35.69 dBi – a decrease of 1.73 dBi. At the same time, it can be observed that the beam broadens slightly when the antenna is mounted in the platform.

B. Side-lobe levels

The side-lobe levels are listed in Table II. It is seen that the side-lobe levels in the two principal planes ($\phi = 0^\circ$

TABLE II

Side-lobe levels (in dB below peak) for antenna alone and antenna mounted in CubeSat platform.

	$\phi = 0^\circ$	$\phi = 45^\circ$	$\phi = 90^\circ$
Antenna	22.54	28.42	27.23
Antenna mounted in platform	17.96	31.59	18.34

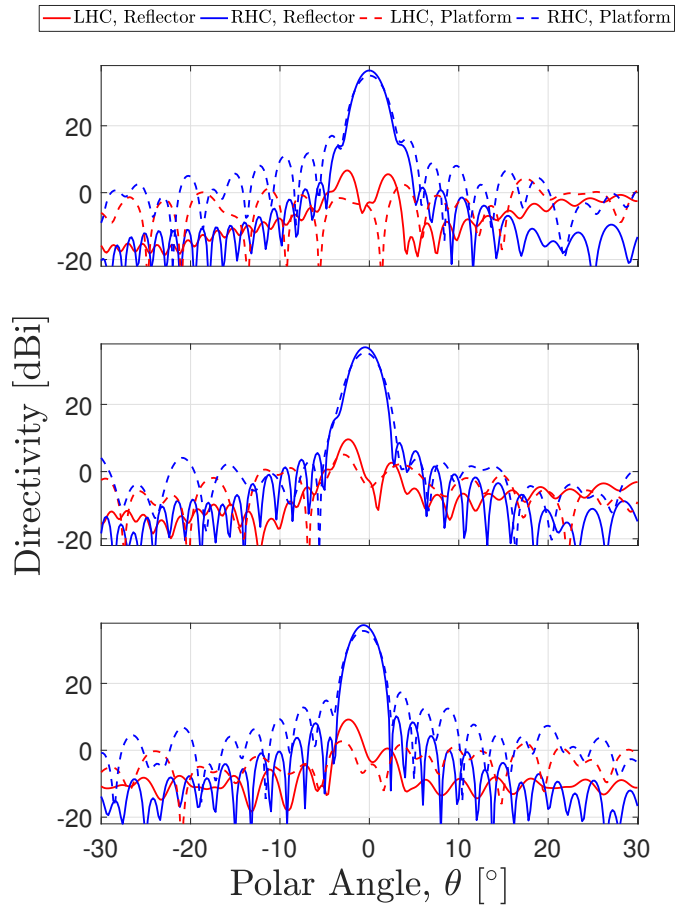


Fig. 3. Directivity patterns. [Blue/red] curves are [RHC/LHC], [solid/dashed] curves are for the reflector [alone/mounted in platform]. The top panel shows pattern cuts in the $\phi = 0^\circ$ cut, the centre shows the $\phi = 45^\circ$ cut, and the bottom shows the $\phi = 90^\circ$ cut.

and $\phi = 90^\circ$) decrease significantly when the antenna is mounted in the CubeSat platform while the side-lobe performance in the $\phi = 45^\circ$ cut is improved.

To further investigate this behaviour, the patterns are plotted in two-dimensional (u, v) -grids in Fig. 4 ($u = \sin(\theta) \cos(\phi)$ and $v = \sin(\theta) \sin(\phi)$). In these plots it is seen that while the side lobes of the antenna alone are circular symmetrical and quickly dies off as we move away from the main beam, the side lobes for the antenna mounted in the CubeSat platform are dominated by two lines of lobes in the principal planes ($u = 0$ and $v = 0$) and are in general more spread out than for the antenna alone.

C. Cross-polar discrimination

As the final parameter, the cross-polar discrimination (XPD) levels are investigated. In Fig. 5, the XPD patterns are plotted in (u, v) grids. The peak XPD values are in both cases better than 40 dB inside the main beam of the antenna.

For the antenna alone we can observe the expected symmetric pattern showing the effects of the beam squint.

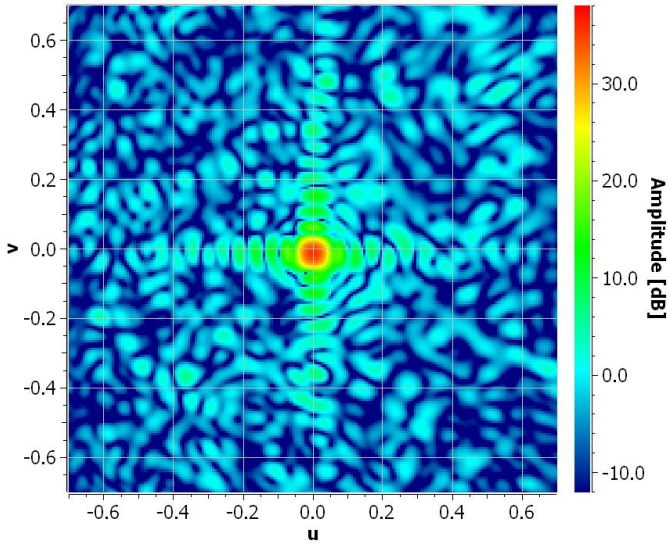
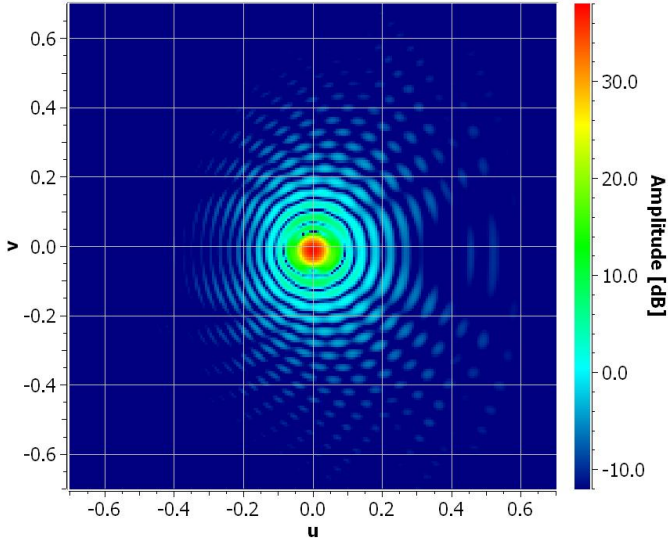


Fig. 4. RHC directivity patterns. Top panel: Antenna alone. Bottom panel: Antenna installed in CubeSat platform.

When the antenna is mounted inside the CubeSat platform, the symmetry of the pattern disappears due to the scattering from the platform. It should also be noted that due to the higher RHC side-lobe levels observed in Fig. 4 for the installed antenna, the XPD values are actually increased in large regions for the installed antenna, as can be seen in the bottom plot in Fig. 5. However, these are all regions where the co-polar level is more than 30 dB below the peak of the main beam.

IV. Conclusion

The performance of an offset reflector operating at 86 GHz was investigated in two configurations: When the antenna is alone and when the antenna is installed in a 6U CubeSat platform. Significant differences in the performance of the antenna were demonstrated, with a

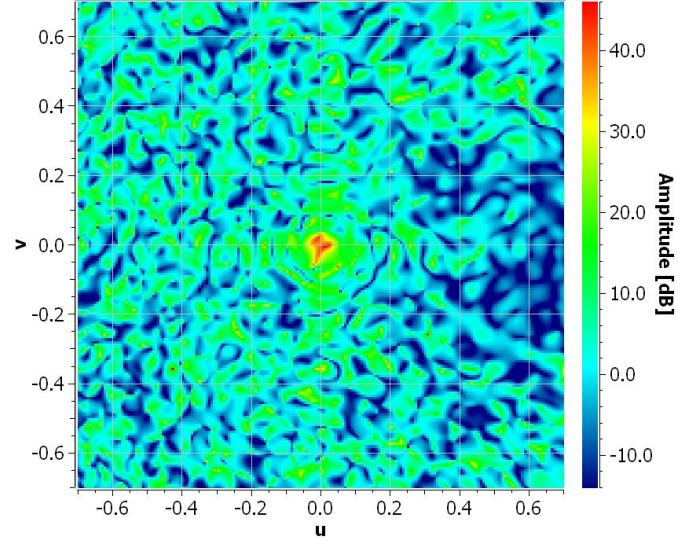
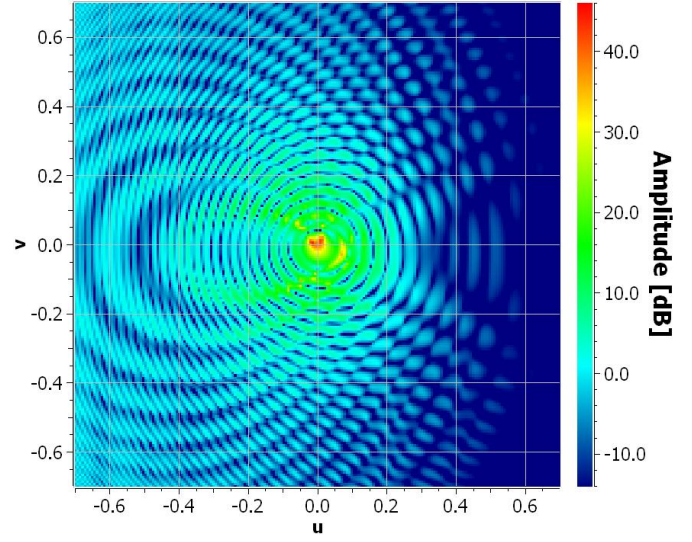


Fig. 5. XPD (RHC/LHC) patterns. Top panel: Antenna alone. Bottom panel: Antenna installed in CubeSat platform.

decrease in peak directivity of 1.73 dB likely being the most mission critical.

The analyses show that as the frequency increases and the antenna system become more complex, it becomes important to take into account the effects of platform scattering in order to achieve accurate predictions of the installed performance of antennas on CubeSat platforms.

References

- [1] The CubeSat Program, California Polytechnic State University, “6u CubeSat Design Specification Revision 1.0,” Jun. 2018.
- [2] ESA’s ARTES Programme, “W-Cube - CubeSat-based W-band channel measurements.” [Online]. Available: <https://artes.esa.int/projects/w-cube>
- [3] TICRA Tools 19.0 Software, TICRA, Copenhagen, Denmark, www.ticra.com.
- [4] E. Jørgensen, O. Borries, P. Meincke, M. Zhou, and N. Vesterdal, “New fast and robust modelling algorithms for electrically large

antennas and platforms,” in 2015 9th European Conference on Antennas and Propagation (EuCAP), April 2015.

- [5] G. Mishra, S. K. Sharma, and J. S. Chieh, “A circular polarized feed horn with inbuilt polarizer for offset reflector antenna for W-band CubeSat applications,” *IEEE Trans. Antennas Propag.*, vol. 67, no. 3, pp. 1904–1909, March 2019.